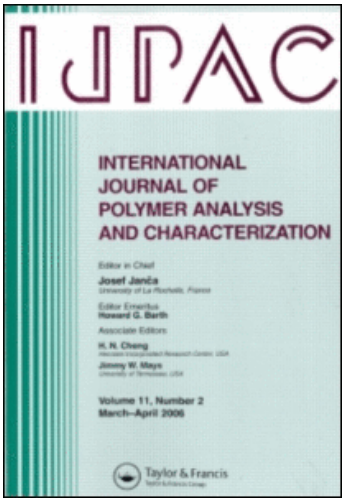

International Journal of Polymer Analysis and Characterization
Publication details, including instructions for authors and subscription information:
http://www.informaworld.com/smpp/title~content=t713646643

SEC Molecular-Weight-Sensitive Detection

Thomas H. Mourey[a]
[a] Imaging Materials and Media, Research and Development Laboratories, Eastman Kodak Company, Rochester, New York, USA

Online publication date: 16 August 2010

To cite this Article Mourey, Thomas H.(2004) 'SEC Molecular-Weight-Sensitive Detection', International Journal of Polymer Analysis and Characterization, 9: 1, 97 — 135
To link to this Article: DOI: 10.1080/10236660490890510
URL: http://dx.doi.org/10.1080/10236660490890510

International Journal of Polymer Anal. Charact., 9: 97–135, 2004

ISSN: 1023-666X print
DOI: 10.1080/10236660490890510

SEC Molecular-Weight-Sensitive Detection

Thomas H. Mourey
Imaging Materials and Media, Research and Development Laboratories, Eastman Kodak Company, Rochester, New York, USA

In addition to an updated view of the basic principles of viscometry and elastic light scattering molecular-weight-sensitive detectors for size-exclusion chromatography (SEC), this review also examines many of the specific applications described in publications since 2001. These include the use of multidetector systems for validating SEC fractionation, examining polymer conformation, quantifying many forms of polymer topology (e.g., branching), physiochemical studies (e.g., phase separation and aggregation), analyzing oligomers, assessing polymer optical anisotropy, and estimating second virial coefficients. Although multidetector SEC is not without sources of error and uncertainty, it has developed into an extremely powerful analytical method that is increasingly used to accomplish diverse and difficult polymer analyses.

Keywords: Size-exclusion; Light scattering; Viscometry; Detection; Multidetector; Polymer; Topology; Conformation

INTRODUCTION

Polymer molecules fractionated by size-exclusion chromatography (SEC) are usually detected in the eluate with an on-line differential

Received 15 December 2003; accepted 11 September 2004.
The author is indebted to Ms. Joan Haslip for her assistance in retrieving much of the literature cited in this review, and to Dr. Charles Lusignan and Ms. Sharon Ryan of Eastman Kodak Company and Prof. Steve Balke from the University of Toronto for reading and commenting on early versions of this manuscript.
Address correspondence to Thomas H. Mourey, Research and Development Laboratories, Eastman Kodak Company, 1699 Lake Ave., Rochester, NY 14650-2136, USA. E-mail: thomas.mourey@kodak.com

refractive index (DRI), spectrophotometric, or other concentration-sensitive detector. The concentration-sensitive detector response can be normalized to calculate the weight fraction of the polymer as a function of elution volume. Although useful for relative comparisons, this normalized chromatogram has limited utility unless elution volume is converted to something more meaningful, such as polymer molecular size or molecular weight. The early years of SEC were limited to measuring retention volumes of polymer standards of known molecular weight and viscosity and constructing calibration curves of $\log M$ or $\log [\eta]M$ versus retention volume for the conversion of the retention volume axis. The limitations of these methods were recognized early, and there soon appeared continuous, on-line detectors that measured dilute polymer solution viscosity[1], elastically scattered light[2], and osmotic pressure[3,4].

Viscometry and elastic light scattering detectors were eventually commercialized and are commonly used today. These detectors are referred to as "molecular-weight-sensitive" because their responses are related in some way to the molecular weight of the eluting species. They are normally used in addtion to a detector that measures polymer concentration, and "multidetector" SEC (sometimes referred to as "triple detection") combines both viscometry and light scattering with one or more concentration-sensitive detectors. SEC with molecular-weight-sensitive detection is used in place of conventional light scattering and viscometry for polymer dilute solution characterization for several reasons: modern high performance liquid chromatography (HPLC) equipment enables accurate, reproducible, and highly automated analyses; the SEC fractionation provides distribution information, whereas conventional methods measure average quantities of the unfractionated polymer; the molecular-weight-sensitive detector measurements are made at constant chemical potential because solvent molecules and salts are separated from the polymer during elution; and the high sensitivity of these detectors permits measurement of polymer properties at each point of the SEC size distribution at highly dilute concentrations.

This review covers the developments in SEC molecular-weight-sensitive detection since 2001. It is not intended to be all-inclusive but, rather, to introduce basic concepts and to provide examples of how the technology is used currently in several areas of polymer characterization. The article has two sections: Detection Principles, with a focus on methods for calculating quantities of interest, and Applications, which includes examples from the 2001–2003 literature. Emphasis is placed on applications that involve more than simple measurement of molecular weight distributions. The reader is also referred to current reviews on the uses of SEC light scattering detectors for the analysis of branched polymers[5] and complex biopolymers[6], a review of multidetector SEC with both viscometry and light scattering detection for complex polymers[7], and new texts on polymer solutions[8], polymer physics[9], and a

chromatography encyclopedia[10] that discuss size-exclusion with molecular-weight-sensitive detection.

DETECTION PRINCIPLES

The operating principles of viscometry and light scattering detectors have not changed significantly in recent years, and the reader is referred to excellent, earlier reviews for details[11,12]. However, the methods used to calculate molecular weight, viscosity, and radii at each point of an SEC chromatogram deserve some discussion. The interpretation of the relationships between these quantities is emphasized in many applications over the past three years, and the calculation methods and their associated assumptions and error have an effect on the elucidation of polymer quantities of interest, such as conformation and topology. Some of the basic equations are presented below. Readers familiar with them can move directly to the Applications section.

Viscometry Detection

Viscometry detectors measure the pressure drop, ΔP, across a capillary of radius r and length l for solution traveling at flow rate Q. The pressure drop is related to the viscosity of the solution through the Hagen-Poiseuille equation,

$$\eta = \frac{\pi r^4 \Delta P}{8lQ} \tag{1}$$

with viscosity in cgs units of poise or SI units of Pascals. The first design for continuous monitoring as an SEC detector used a single capillary[1]. Single capillary instruments are extremely sensitive to flow rate variations, which prompted the development of multiple capillary and pressure transducer designs that simultaneously measure the polymer solution in one part of the detector and pure solvent in another. Multiple capillary[13,14] and differential bridge[15] configurations were eventually commercialized. Schematics of commercially available models appeared in a recent review[16], and comparisons of designs were made in some detail previously[17]. The specific viscosity is calculated at each elution point i at constant flow rate,

$$\eta_{sp,i} = \frac{\eta_i - \eta_0}{\eta_0} \tag{2}$$

where η_0 is the viscosity of the solvent. Values at each elution point are referred to as "local values," in this case, the local specific viscosity. Depending on configuration, specific viscosity is calculated differently

from pressure measurements. For example, with a single capillary, the specific viscosity is:

$$\eta_{sp,i} = \frac{P_i - P_0}{P_0} \tag{3}$$

where P_i is the pressure at each elution point i for the sample solution, and P_0 is the pressure drop for pure eluent. Bridge models measure a differential pressure, P_{diff}, between a sample solution flowing through capillaries and solvent flowing through a second set of capillaries matched to the sample set, analogous to a Wheatstone bridge. The specific viscosity is obtained from the differential pressure and the pressure drop across the entire bridge, referred to as the inlet pressure, P_{in}:

$$\eta_{sp,i} = \frac{4P_{diff}}{P_{in} - 2P_{diff}} \tag{4}$$

Specific viscosity is unitless and can be combined with concentration at each elution point, c_i, often measured by a differential refractive index detector, to provide the local reduced viscosity, $\eta_{red,i}$:

$$\frac{\eta_{sp,i}}{c_i} = \eta_{red,i} \tag{5}$$

The local intrinsic viscosity is the local reduced viscosity at the limit of zero concentration:

$$\lim_{c \to 0} \eta_{red,i} = [\eta]_i \tag{6}$$

Reduced and intrinsic viscosity have units of inverse mass concentration, usually either dL/gm or cm^3/gm. SEC sample concentrations are quite low and the error introduced by assuming that the intrinsic viscosity is equal to the reduced viscosity is usually negligible, although the approximation below is sometimes used to correct for finite concentration[14]:

$$[\eta]_i^* = \frac{\sqrt{2[\eta_{sp,i} - \ln(\eta_{sp,i} + 1)]}}{c_i} \tag{7}$$

Brun provided further details in a recent summary of the determination of intrinsic viscosity by SEC-viscometry detection[18].

The viscometry detector, combined with a concentration detector, directly provides an intrinsic viscosity distribution[19]. The concentration

detector response is normalized by dividing the chromatogram heights, W_i, by the area under the concentration chromatogram, where Δv_i is the volume increment between data points:

$$W_{N,i} = \frac{W_i}{\sum_{i=0}^{i=j} W_i \Delta v_i} \tag{8}$$

The normalized intrinsic viscosity distribution is then obtained in a manner analogous to differential molecular weight distributions,

$$W_{N,i}(\log[\eta]) = -W_{N,i} \frac{dV}{d\log[\eta]} \tag{9}$$

where $d\log[\eta]/dV$ is the slope of the $\log[\eta]$ versus retention volume (V) calibration curve. The whole polymer intrinsic viscosity may also be obtained without the concentration detector response by integrating the specific viscosity chromatogram and from the mass of sample injected, m_t:

$$[\eta] = \frac{\sum_{i=1}^{i=j} \eta_{sp,i} \Delta v_i}{m_t} \tag{10}$$

Viscometry detectors rely on the validity of universal calibration to calculate molecular weight distributions. The calibration curve is constructed from polymers of known molecular weight and intrinsic viscosity (which can be measured by the viscometry detector when running the narrow standards and use of Equation (10)) and plotted as the logarithm of hydrodynamic volume, $J_i = [\eta]_i M_i$, versus retention volume. The local intrinsic viscosity obtained from the viscometry and concentration detectors and application of Equations (5)–(7) is used with the universal calibration curve to calculate the molecular weight at each elution point. This is a number-average molecular weight, $M_{n,i}$[20], if a mixture of molecules of equivalent sizes exists:

$$\log M_{n,i} = \log J_i - \log[\eta]_i \tag{11}$$

Also, the number-average molecular weight of the whole polymer may be obtained from the specific viscosity chromatogram and the universal calibration curve, without the use of a concentration detector[21,22]:

$$\overline{M}_n = \frac{m_t}{\sum_{i=1}^{i=j} \frac{\eta_{sp,i}}{[\eta]_i M_i} \Delta v_i} \tag{12}$$

It is possible to estimate the radius of gyration at each elution point, $R_{g,i}$, from the hydrodynamic volume $M_i[\eta]_i = J_i$ obtained from the universal calibration curve and the Flory-Fox equation:

$$R_{g,i} = \frac{1}{\sqrt{6}} \left(\frac{M_i[\eta]_i}{\Phi} \right)^{1/3} \tag{13}$$

where

$$\Phi = 2.55 \times 10^{21}(1 - 2.63\xi + 2.86\xi^2) \tag{14}$$

and

$$\xi = \frac{2a - 1}{3} \tag{15}$$

The exponent of the Mark-Houwink relationship, $[\eta] = K_a M^a$, can be obtained from the SEC-viscometry detection. This approach provides reasonable estimates for some linear polymers[12] such as in a recent application to poly(ε-carprolactone)s[23], but is of limited utility because the assumptions underlying Equations (13)–(15) may not hold for other polymer topologies.

Elastic Light Scattering Detection

Elastic light scattering SEC detection for continuous measurement of excess Rayleigh scattering dates to a 1974 low-angle design[2]. The basic light scattering equation relating excess Rayleigh scattering, $R(\theta)_i$, at angle θ from the incident beam, and the local weight-average molecular weight $M_{w,i}$, and concentration c_i,

$$\frac{K_i c_i}{R(\theta)_i} = \frac{1}{M_{w,i} P(\theta)_i} + 2A_{2i}c_i + \cdots \tag{16}$$

takes the simple form

$$M_{w,i} = \frac{R(\theta)_i}{K_i c_i} \tag{17}$$

assuming that the second virial term $2A_{2i}c_i$ is negligible at the low concentrations employed in SEC and that the particle scattering function $P(\theta) \sim 1$ at low angles for polymer sizes that can be fractionated by SEC

columns. The optical constant K_i for vertically polarized incident and collected light contains the solvent refractive index, n, polymer specific refractive index increment dn/dc, Avogardo's number N_A, and the wavelength of light in vacuum, λ_0.

$$K_i = \frac{4\pi^2 n^2 (dn/dc)_i^2}{N_A \lambda_0^4} \tag{18}$$

For collection of scattered light through an annular opening such as in some low-angle instruments,

$$K_i = \frac{2\pi^2 n^2 (dn/dc)_i^2 (1 + \cos^2\theta)}{N_A \lambda_0^4} \tag{19}$$

Equation (17) applies for measurement at any angle, but the assumption $P(\theta) \sim 1$ is reasonable only for progressively smaller polymer molecules as the angle increases for a fixed K_i. An iterative method for estimating $P(\theta)$ and R_g from light scattering detection at $\theta = 90^\circ$ combined with viscometry detection and universal calibration[24] is used in some commercial software. Again, the approach is limited to the applicability of Equation (13) for some linear polymers.

The angular variation of scattered light is measured with multi-angle light scattering (MALS) instruments[25]. The particle scattering function is commonly given in the form of a power series in scattering vector, q:

$$\lim_{c \to 0} \frac{K_i c_i}{R(\theta)_i} = \frac{1}{M_{w,i}} \left[1 + \frac{1}{3} q^2 R_{g,i}^2 + \cdots \right] \tag{20}$$

$$q = \frac{4\pi n}{\lambda_0} \sin\left(\frac{\theta}{2}\right) \tag{21}$$

Equation (20) can be applied in the analysis of MALS data using reciprocal scattering plots of Zimm[26] in which the limiting slope at zero angle is proportional to the radius of gyration and the intercept is $1/M_{w,i}$. This solution for $P(\theta)$ becomes independent of the shape of the polymer molecule as θ approaches zero. Alternative plotting methods[27] may improve the estimate of $R_{g,i}$ and were evaluated recently with regard to accuracy and robustness[28].

Light scattering detectors that use one low angle (usually 15°) and a second angle at 90° are not suited for graphical methods based on Equation (20). For anisotropic scatterers, the ratio of the scattering

intensities, Z_i, at angles θ_1 and θ_2 is equal to the ratio of the particle scattering functions at these two angles[29,30].

$$Z_i = \frac{P(\theta_1)_i}{P(\theta_2)_i} = \frac{R(\theta_1)_i}{R(\theta_2)_i} \tag{22}$$

Analytical solutions for particle scattering are available for a number of shapes, including random coils, spheres, rods, and rings[31], which are used to calculate $P(\theta)_i$ and $R_{g,i}$ as a function of Z_i. The method measures accurate molecular weights and radii of gyration for linear and branched polymers separated on high-performance SEC columns[32]. On such columns, the particle scattering factors for various topologies differ little up to the maximum practical size that can be separated. The assumption of a particle shape becomes more important for ultrahigh molecular weight polymers separated on low-shear, large particle diameter columns.

The intrinsic viscosity can be estimated from M_i and $R_{g,i}$ from light scattering detection at more than one observation angle and Equations (13)–(15)[33]. Again, inherent assumptions in the calculation limit applicability to some linear polymers, and this is not considered as a substitute for the actual measurement of local intrinsic viscosities by a viscometry detector.

Recently, dynamic light scattering (DLS) has become available as an on-line SEC detector. DLS measures the time dependence of scattered light intensity fluctuations, which depends on self-diffusion of the macromolecules. The detectors are used primarily to measure hydrodynamic size rather than molecular weight and, as such, are not "molecular-weight sensitive" in the same sense as elastic light scattering and viscometry detectors. The operation principles and data analysis methods for DLS detection are conceptually different from elastic light scattering detection and will not be covered here further. Although only a few articles have appeared on operating principles[34,35] and the use of SEC-DLS for proteins[36] and polymers[37,38] in the past two years, the emergence of SEC-DLS is noteworthy because the detectors integrate with elastic light scattering, viscometry, and concentration detectors into "multidetector" SEC systems. Such systems can potentially measure several relationships between sizes and mass simultaneously, which has been an active topic in the past three years and is discussed later in this review.

Sources of Error

The dependencies of detector signal intensity, I, on molecular weight and concentration can be expressed as a power law, $I = f(M^{\gamma}, c)$, for common SEC detectors:

DRI	$\Delta n_i \sim c_i(dn/dc)_{i,M>10k}M^0$	$\gamma = 0$	(23)
Viscometry	$\eta_{sp,i} = c_i K_a M^a$	$\gamma \sim 0.33-1.0$	(24)
Light scattering	$R(\theta)_i = Kc_i P(\theta) M_i$	$\gamma = 1$	(25)

This formalism also puts mass spectrometry and spectrophotometric detection selective for end groups in perspective because both are molar detectors:

$$I_i = N_i = c_i/M_i \qquad \gamma = -1 \tag{26}$$

Molar detectors are more sensitive to the smallest molecules in a molecular size distribution and may be more useful than light scattering and viscometry for measuring quantities that are sensitive to the number of smaller molecules, such as the number-average molecular weight. The dependencies given by Equations (23)–(25) explain mismatched signal intensities at early elution times, where light scattering and viscometry detectors have more response than the concentration detector, and vice versa, at long elution times. This presents regions of the chromatograms where the local intrinsic viscosity or local weight-average molecular weight cannot be calculated because either the concentration or molecular-weight-sensitive detector signal is too weak to measure. Some data analysis methods estimate the intrinsic viscosity and molecular weight in regions of weak signal response by model fitting or weighted extrapolations[39,40]. The methods have inherent limitations that are only as good as the raw data. The best strategy for minimizing errors introduced from mismatched detector signals is to minimize the region of mismatch by maximizing detector signal-to-noise ratio. The best gains are from improved chromatography with solvents and columns, stable pumping systems, and optimized sample concentrations.

The mismatched detector sensitivity problem is well known and appreciated, even with optimized chromatographic conditions. A recent approach was designed to provide more accurate measurement in the short retention volume (high molecular weight) regions of chromatograms where DRI signals are weak[41]. The method uses the signals from a light scattering detector and molecular weights at each elution point from a preestablished log M versus retention volume calibration curve of the polymer of interest. It was evaluated for the measurement of M_z values, which were correlated with the melt rheology of polyethylenes. The general form for calculation of molecular weight averages is

$$M_q = \frac{\sum w_i M^{q-1}}{\sum w_i M^{q-2}} = \frac{\sum LS_i M^{-2}}{\sum LS_i M^{-3}} \tag{27}$$

where the light scattering signal is proportional to sample weight concentration, w_i, and weight-average molecular weight at each elution point $LS_i = w_i M_{w,i}$, and $q = 2$, 3, and 4 for M_w, M_z, and M_{z+1}, respectively. In this example, high-density linear polyethylenes were examined, and a calibration curve was constructed from narrow standards and Mark-Houwink constants. The method might provide improved estimates of averages obtained from higher distribution moments such as M_z and M_{z+1}. In the case of branched polymers or unknown topology or composition, the method can be used for relative comparisons with improved precision, but the molecular weight averages may not be equal to the true molecular weight values.

The volume delay between molecular-weight-sensitive detectors and the concentration detectors must be known to combine the signals for calculation of local intrinsic viscosity and weight-average molecular weight. Small errors in the interdetector volume rotate light scattering log M and viscometry log $[\eta]$ versus retention volume calibration curves and introduce nonlinearity and unusual curve shapes. Nonlinear calibration curves can also be obtained when axial dispersion exists. The problem becomes more acute with narrow distributions and, in many instances, "N"-shaped calibration curves are obtained, which is a common result of different degrees of extra-column band broadening in the molecular-weight-sensitive and concentration detectors. The effects of axial dispersion on the local, uncorrected intrinsic viscosity $[\eta]_{i,uc}$ measured by viscometry detection are often corrected ($[\eta]_{i,c}$) by the method of Hamielec[42],

$$\log[\eta]_{i,c} = \log[\eta]_{i,uc} + \log\left[\frac{c_i}{c_{i-D_{2\eta}\sigma^2}}\right] - \frac{(D_{2\eta}\sigma)^2}{4.606} \tag{28}$$

where c_i is the concentration at elution point i, $D_{2\eta}$ is the slope of the ln $[\eta]$ versus retention volume calibration curve, and σ is the standard deviation band spreading parameter. A similar correction can be applied to the local weight-average molecular weights obtained from light scattering detection:

$$\log M_{i,c} = \log M_{i,uc} + \log\left[\frac{c_i}{c_{i-D_2\sigma^2}}\right] - \frac{(D_2\sigma)^2}{4.606} \tag{29}$$

where D_2 is the slope of the ln M versus retention volume curve. For narrow distribution standards, these corrections can yield marginal results. The author's experience is that much of the problem is eliminated

by minimizing $D_2\sigma$ and $D_{2\eta}\sigma$, as described by Jackson and Yau[43]. This typically involves use of high-efficiency columns that minimize axial dispersion and by selecting a column set with a large total column volume. Both interdetector volume and axial dispersion have been the subject of continued investigation[44,45,46] in the past three years. These sources of error affect more than the accuracy of molecular weight distributions; both interdetector volume error and axial dispersion have large effects on double logarithmic plots such as those shown in Figures 1 and 2. Such plots have appeared frequently in the literature over the past three years, and conclusions drawn from their shapes and slopes require care and consideration of potential errors introduced by interdetector

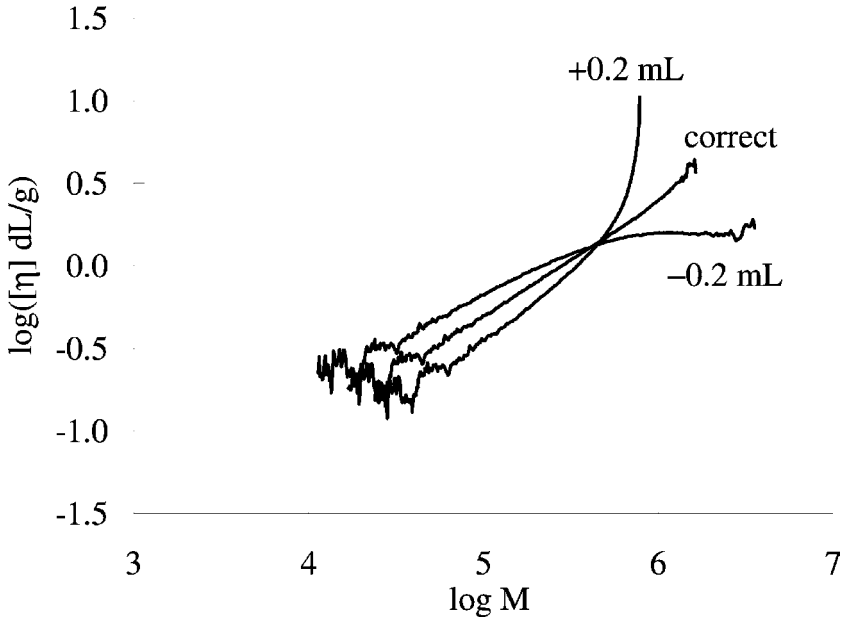

FIGURE 1 Effects of interdetector volume error on viscosity – molecular weight conformation plots. Broad molecular-weight distribution polystyrene, 0.100 mL injection of 1.5 mg/mL sample solution, separated on three Polymer Laboratories Mixed-C columns in tetrahydrofuran at a flow rate of 1.0 mL/min. The viscometry detector and DRI are arranged with a parallel split and the effective interdetector volume is near zero mL. The top curve results from calculating the local intrinsic viscosities and molecular weights by setting the interdetector volume at +0.2 mL and the bottom curve from an interdetector volume of −0.2 mL.

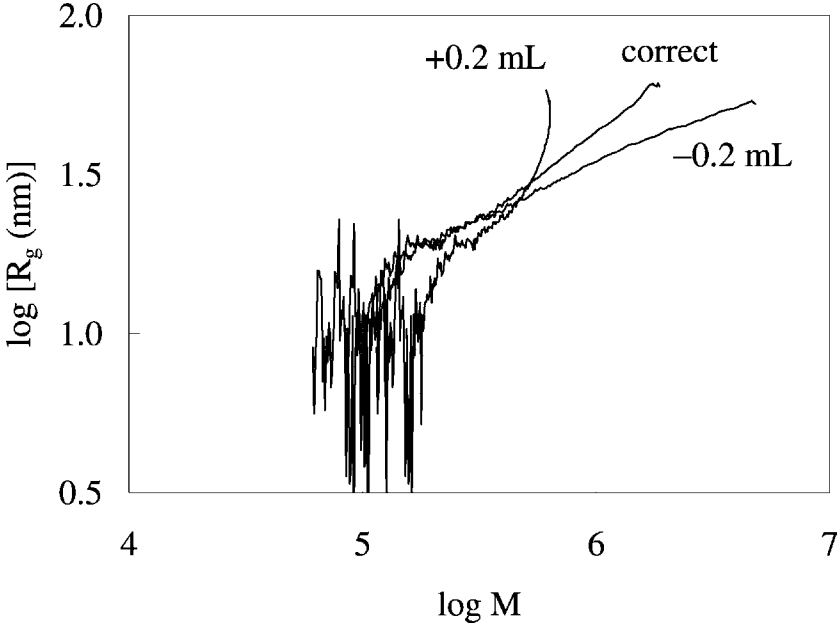

FIGURE 2 Effects of interdetector volume error on radius of gyration – molecular weight conformation plots. Same experimental conditions as Figure 1. The two-angle light scattering detector is connected before the DRI in a serial arrangement.

volume, axial dispersion, and extrapolations made to compensate for mismatched detector sensitivity.

APPLICATIONS

Validating SEC Fractionation

Molecular-weight-sensitive detectors are useful in detecting non-exclusion effects in a size-exclusion separation. For example, light scattering detection was used recently on cationic methacrylate-acrylate copolymers[47] to find conditions that minimized adsorptive interactions. Other recent examples include highly branched styrene-divinylbenzene polymers[48] and poly[(diphenoxy)phosphazene][49] that exhibited late elution. Upturns in the long retention volume region of log M versus retention volume plots or in the low molecular weight region of log R_g versus log M conformation plots obtained from MALS detection indicated that

large molecules eluted later than expected for a true size separation. Given the potential for error in conformation plots caused by uncertainties in interdetector volume and axial dispersion, the first comparision is considered more reliable. The use of both viscometry and light scattering detection provide further insight into non-exclusion behavior or SEC artifacts, particularly for high molecular weight materials such as hyaluronans[50], which can be problematic for many SEC columns. Comparisons of the log M versus retention volume calibration curves obtained directly from light scattering detection and indirectly from viscometry detection and the universal calibration curve are particularly valuable. In the case of late elution, the calibration curves diverge in the regions of late elution (Figure 3) and also diverge in the regions of short retention volume in the case of shear degradation (Figure 4). Such information is helpful in the selection of column materials, frits, and experimental conditions, as shown recently for ultrahigh molecular weight polyolefins[51] and polystyrenes[52].

Error in the total mass injected can also be recognized from the log M versus retention volume calibration curves obtained from viscometry and

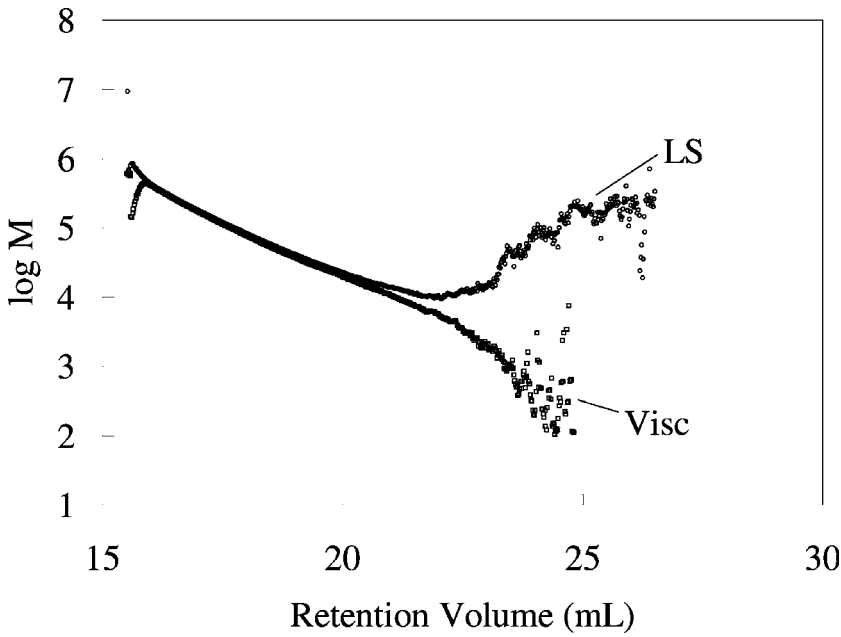

FIGURE 3 Example of log M vs. retention volume curves obtained from light scattering and viscometry detection for a sample exhibiting late elution. Same experimental setup as Figures 1 and 2.

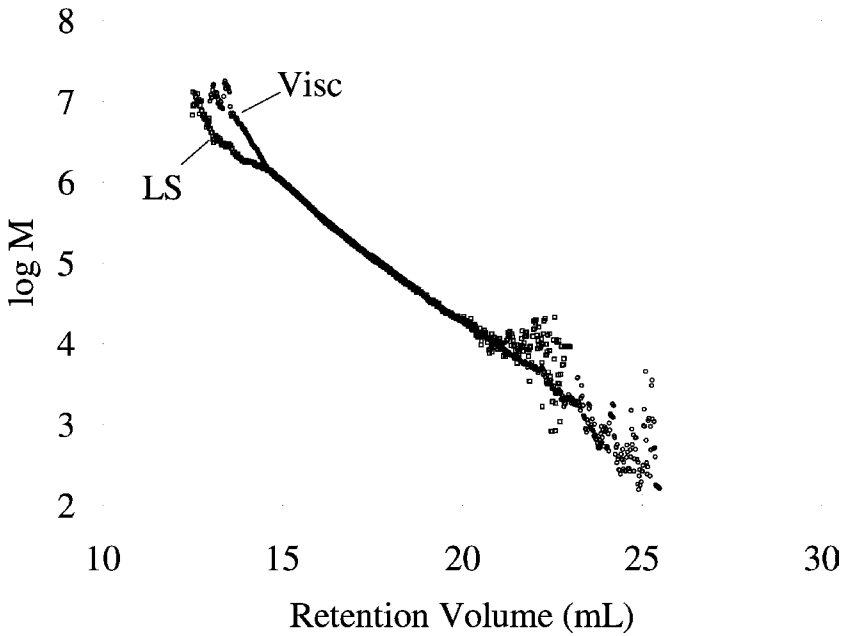

FIGURE 4 Example of log M vs. retention volume curves obtained from light scattering and viscometry detection of a sample undergoing shear degradation. Same experimental setup as Figures 1 and 2.

light scattering. The error might be introduced during sample weighing or dilution, from error in the injection volume, or by unknown amounts of residual solvent, monomer, or filler that are mistakenly assumed to be part of the polymer sample. One outcome is disagreement in the log M calibration curves obtained directly from light scattering detection and the same calibration curve obtained from viscometry detection and the universal calibration curve. When the concentration is estimated low, the viscometry log M calibration curve will be displaced to lower values than the light scattering log M values. The opposite displacement occurs for a concentration that is erroneously high. A similar discrepancy in calibration curves will be observed if the specific refractive index increment is incorrect for light scattering calculations.

Mixtures of molecules differing in chemical composition but having the same hydrodynamic size can introduce a related source of error. In such instances, the molecules elute at the same SEC retention volume, and each elution slice is said to have local polydispersity. If the chemically different species have different concentration detector responses, error is introduced in the calculation of the local concentration, c_i, at each elution

point of the chromatogram, which subsequently affects the calculation of the local molecular weight by light scattering detection and the local intrinsic viscosity by viscometry detection. Recently, three methods for detecting local polydispersity were evaluated[53]. The first is the comparison of $\log M$ versus retention volume calibration curves from light scattering and viscometry detection. Disagreement occurs in regions where a mixture of molecules with different specific refractive index increments coexists. A second method involves reconstruction of DRI concentration chromatogram response, W_i^*, from the light scattering and viscometry detector responses and the universal calibration curve, J_i,

$$W_i^* = \beta\left(\frac{\eta_{sp}R(\theta)_i}{\alpha P(\theta)_i J_i}\right)^{\frac{1}{2}} \tag{30}$$

where α is the light scattering optical constant not containing dn/dc and β is a DRI response constant. The reconstructed chromatogram is compared to the experimental DRI chromatogram response, W_i, and if differences are observed, local polydispersity is present. A third method by Brun[54] reconstructs the universal calibration curve from the viscometry, light scattering, and concentration detector responses,

$$J_i^* = \beta^2\left(\frac{\eta_{sp}R(\theta)_i}{\alpha P(\theta)_i W_i^2}\right) \tag{31}$$

Differences between the reconstructed (J_i^*) and actual (J_i) universal calibration curves again indicate the presence of local polydispersity. The ability of the three methods to detect local polydispersity is limited by the difference in specific refractive increments of the different components and their relative amounts. If local polydispersity is detected, cross fractionation may be appropriate. In the case of mixtures of polymers with different chemical composition, methods that use a concentration detector that is selective for one component, along with the DRI, may be suitable[55]. For block copolymers, if the molecular weight of the first block is known or easily measured, a new method that uses only a DRI and a UV detector that is selective for one block component can be applied[56].

A final example involves validating universal calibration with both light scattering and viscometry detection. Sodium trifluoroacetate (NaTFA) has been added to 1,1,1,3,3,3-hexafluoro-2-propanol (HFIP), since introduced by Drott[57], to suppress anomalous SEC behavior – particularly prepeaks that were assumed to be molecular aggregates. A recent study showed that different universal calibration curves are obtained with HFIP/NaTFA for poly(methyl methacrylate) (PMMA), poly(ethylene oxide) (PEO), and poly(2-vinylpyridine) (P2VP)

standards[58]. Replacement of NaTFA with tetraethylammonium nitrate (TEAN) increases retention volumes of all standards and results in superimposed universal calibration curves. The intrinsic viscosities and radii of gyration PMMA, poly(ethylene terephthalate) (PET), and nylon 6,6 are the same regardless of the amount of NaTFA or TEAN added, suggesting that one role of the added electrolyte is to suppress repulsive interactions with the column packing. In addition, PEO and P2VP undergo conformational changes in the presence of TEAN, resulting in smaller radii and lower intrinsic viscosities. The net result of TEAN is to provide superimposed universal calibration curves at concentrations greater than 0.01 M. This eliminates the need for "artificial" calibration curves to improve molecular weight estimates of polyamides in HFIP with potassium trifluoroacetate[59].

Conformation

The spatial structure or conformation of a polymer chain is determined by the relative location of its monomer units. In dilute solution, the conformations that a chain adopts depend on the flexibility of the chain, the interactions between monomers on the chain, and interactions with the surroundings, such as solvent and other macromolecules. Examples of common conformations observed in dilute solution include compact spheres, swollen random coils, and rigid rods.

The exact spatial locations of the monomers in a polymer chain evolve over time as the molecules move throughout their environment because of Brownian motion. In a macroscopic sample, identical molecules of the same length can have distributions of monomers that are different, and identical molecules of the same size comprise different numbers of monomers. Polymer properties are thus by nature "average quantities," representing the aggregate response of many molecules. The tools of statistical mechanics are used to calculate relevant quantities. Experimentally, the average conformations present in a sample are determined by measuring the relationship between the sizes of macromolecules and the distribution of mass within that size–quantities that are obtained by SEC with molecular-weight-sensitive detection. The ratio of a molecule's spatial size to its molar mass forms the basis of polymer conformation analysis. Of primary importance is the scaling relationship between radius of gyration and molecular weight, available from light scattering detection:

$$R_g = K_v M^v = K_v M^{1/d_f} \tag{32}$$

The Flory exponent υ, or equivalently its reciprocal, the fractal dimension of the object, d_f, varies with all the factors that influence conformation, in

particular, molecular architecture and solvent quality. In an SEC-LS experiment, they are obtained from a plot of log $R_{g,i}$ versus log M_i. The fractal dimension provides an intuitive way to characterize the size-to-mass distribution within an object: a linear rod is one-dimensional with $d_f = 1$; a flat disc is two dimensional with $d_f = 2$; and a solid sphere is three-dimensional with $d_f = 3$. Viewed from outside of the polymer, a random coil in solution may appear to be a three-dimensional object, but locally it resembles a one-dimensional thread. Thus, its fractal dimension falls somewhere between one and three, with a value of $d_f = 1.7$ in good solvent and $d_f = 2$ in poor solvent. Chain architecture is reflected in the fractal dimension as well; a randomly branched, freely swollen molecule in a good solvent has a value of $d_f = 2.0$.

A fundamental property of polymers is that their structure is independent of length scale for sizes larger than a few monomer dimensions (the Kuhn length). Thus, any subsection of a polymer chain exhibits the same spatial size-to-molar mass relationship as the entire chain. The molecule is said to be "self-similar." The importance of self-similar objects described by fractal dimensions is that they exhibit power law behavior independent of the length scale used to express the radius of gyration. Thus, the exponent of Equation (32) is universal for polymers with the same conformation, whereas the prefactor K_v varies for polymers within the same conformation class. Similar inferences are obtained from log M versus log[η] Mark-Houwink plots from SEC-viscometry:

$$[\eta] = K_a M^a = K_a M^{3/d_f - 1} \tag{33}$$

Double logarithmic plots of radius of gyration or intrinsic viscosity versus molecular weight are referred to as conformation plots and are obtained directly from SEC-molecular-weight-sensitive detection. Curvature in conformation plots is due to a change in the fractal dimension as a function of molecular weight and indicates that the molecules are significantly different across the molecular weight distribution. An example of this type of conformational change across a distribution occurs in long-chain branched samples where the molecules are linear at small molecular weights and highly branched at larger ones. In some systems, this crossover between linear and branched polymers seen on conformation plots has been used to estimate the chain length between branch points[60].

On-line SEC detection provides both an enormous time savings and an improvement in the quality of information compared to classical analyses of carefully prepared fractions, and it is rapidly replacing the latter method for elucidating conformation. Conformation studies in 2001–2003 covered a remarkable diversity of polymer structures and classes. Examples include polyethylene, polypropylene, polystyrene, and poly (dimethylsiloxane) at 150°C in trichlorobenzene[38], polyphosphazenes[49],

water-insoluble glucan[61], pachyman[62], poly(alkyl *n*-alkylsilane)s[63], amylose and starch[64], glutenin polymers[65], a conjugate between a polymeric drug carrier and the antitumor drug camptothecin[66], partially oxidized polygluronate[67], acacia gum dispersions[68], amylopectins[69], poly(N-vinylcarbazole) and its copolymers with methyl methacrylate[70], cellulose[71], exopolysaccharides[72,73], chemically degraded hyaluronic acid[74], β-cyclodextrin and N-acylurea hyaluronam derivatives[75], extracellular carbohydrate polymers[76] and polysaccharides from mycelium[77], methylhydroxyethylcelluloses[78], hydroxypropyl cellulose[79], polysaccharide-protein complexes from *Ganoderma tsugae*[80], ten yam (*Dioscorea*) starches[81], gelatin and acid-soluble collagen[82], and carboxymethylated derivatives of β-glucan[83].

Poly(N-vinylcarbazole) in a good organic solvent and in a system under theta conditions that is formed by poly(vinylpyrrolidone) in water containing 0.01 M $NaNO_3$ provides examples of the use of SEC-LS for the estimation of molecular dimensions, scaling law coefficients, and unperturbed dimensions that are compared to theoretical models[84]. Similarly, SEC-LS was also combined with molecular dynamics modeling to elucidate conformation, unperturbed dimensions, and characteristic ratios of guar gum[85]. Application of SEC-LS to rod-like poly(γ-benzyl-α-L-glutamate) and poly(γ-stearyl-α-L-glutamate) homopolymers[86] and chitosan[87] estimated the intrinsic persistence length from the radius of gyration using a worm-like chain model. This estimate of chain stiffness was hampered in the case of polyglutamates because of nonlinearity in the conformation plots obtained from narrow distribution samples, possibly suggesting complications introduced by interdetector volume uncertainty and axial dispersion.

The calculation of persistence lengths for chitosans also takes into account the electrostatic persistence length contribution and an electrostatic excluded volume coefficient, which are calculated at each M at different salt concentrations. This treatment indicated that persistence length remained constant for heterogeneous chitosans with low degrees of acetylation, and it increased moderately for homogeneous samples with increasing degrees of acetylation. In another study of chitosans, SEC-MALS was used with ultracentrifuge and viscometric data to elucidate conformation that was between a rod and a coil[88]. Persistence length estimates were also made for degraded β-D-glucan fractions from *Lentinus edodes* from SEC-LS[89], and the molecular weights of fractions in aqueous solution were approximately three times the molecular weight of the same fractions in random coil conformation in dimethylsulfoxide (DMSO), suggesting triple helix conformation in water. Finally, persistence lengths of hyaluronans were calculated from radii of gyration measured by multi-angle light scattering detection and from the molecular weight dependence of intrinsic viscosity obtained from viscometry detection[90]. The viscosity conformation plots were distinctly nonlinear

compared to radius of gyration conformation plots, but the estimates of persistence lengths from the two data sets were similar.

The effects of side groups on the conformation of polysiloxanes was studied by SEC-MALS in toluene and benzene[91]. The slopes of conformation plots were strongly dependent on side group size and flexibility. Poly(dimethylsiloxane) and poly(diethylsiloxane) demonstrated dilute solution behavior of random coils in good solvents. Poly(methylphenylsiloxane) exhibited rigid rod conformation, while poly(methylhexylsiloxane) and poly(methylhexadecylsiloxane) showed speherical (compact) conformation in both solvents.

The effects of short-chain branching on the coil dimensions of polyolefins were studied using both light scattering and viscometry detection[92]. Two new parameters, g_{SCB} and g'_{SCB}, were introduced to express the effect of short-chain branching on the chain dimensions and intrinsic viscosity of copolymers of ethylene with propene, butene, hexene, and octene,

$$g_{SCB} = \frac{R_g^2}{(R_g^2)_L} \tag{34}$$

$$g'_{SCB} = \frac{[\eta]}{([\eta])_L} \tag{35}$$

with the comparisons made to the radius of gyration($(R_g^2)_L$ and intrinsic viscosity $([\eta])_L$ of linear polyethylene at the same molecular weight. Conformation plots were approximately parallel for the different copolymers, and the ratios varied linearly with molecular weight with slopes that depended on the comonomer type.

Topology

Topology refers to the molecular architecture of polymer chains. Examples include linear macromolecules, combs, stars, randomly branched polymers, rings, dendrimers, and hyperbranches. Chains of identical molecular weight could have quite different radii, depending on their topology and, as in conformation analysis, the interrelationships between molecular weight and various radii are useful for elucidating topology. In addition to the radius of gyration, which is a geometrical measure of the radius based on the center of gravity of the molecule in solution, three other radii are useful. The hydrodynamic radius is an equivalent sphere radius that depends on the interaction of the polymer molecule with solvent. This radius increases as the degree of penetration of solvent into the polymer chain decreases (draining decreases), as might be the case for

highly branched polymers. R_h can be measured by DLS detection. The ratio R_g/R_h has theoretical predictions for a variety of polymer architectures and solvent conditions, and decreases from values near 1.8 for self-avoiding coils to 0.778 for a homogeneous hard sphere, with intermediate values for various branched topologies[93]. The ratio R_g/R_h is not a unique characteristic for topology, however, because it also depends on the effects of solvent on chain conformation. Recent results from combined SEC-LS and DLS detection for poly(dimethylsiloxane) (PDMS) in a poor solvent (trichlorobenzene at 150°C) measured $R_g/R_h = 1.27$[38].

The viscometric radius is available from viscometry detection,

$$R_\eta = \left(\frac{[\eta]M}{(10\pi/3)N_A}\right)^{\frac{1}{3}} \tag{36}$$

It differs from the hydrodynamic radius in that the molecule is exposed to a shear gradient and, in most instances of SEC-viscometry detection, approximates R_h. The thermal radius

$$R_T = \left(\frac{3A_2M^2}{16\pi N_A}\right) \tag{37}$$

is, in theory, obtainable from SEC-LS by measurement of the second virial coefficient. The thermal radius depends on the interpenetration of polymer chains. Like the hydrodynamic and viscometric radii, it depends on the segment density of the macromolecule and becomes larger as polymer density increases, as might be the case for highly branched molecules. Its basis is quite different than the hydrodynamic radius, however, because it depends on excluded volume of polymer segments as macromolecules encounter each other, while the hydrodynamic radius depends on the ability of solvent molecules to drain from the macromolecule. The thermal radius has not been measured across a broad molecular weight distribution by SEC-LS, partly because of difficulties discussed later in this article with measuring A_2 with molecular-weight-sensitive SEC detection.

Generalized ratios of the various radii eliminate the molecular weight dependence, and the effects of chain topology can sometimes be more evident. However, generalized ratios measured on unfractionated samples are complicated by polydispersity, which effectively makes R_g/R_h of broad molecular weight distribution, randomly branched polymers indistinguishable from linear polymers (for an explanation, see[93]). The polydispersity of each SEC chromatogram slice is usually narrow–even for branched polymers–therefore, this complication is avoided. The ratio R_g/R_η for linear polystyrene measured by SEC with molecular-weight-sensitive detection (Figure 5) is near the value of 1.25 for linear polyisoprene in a good solvent but may be lower than other values

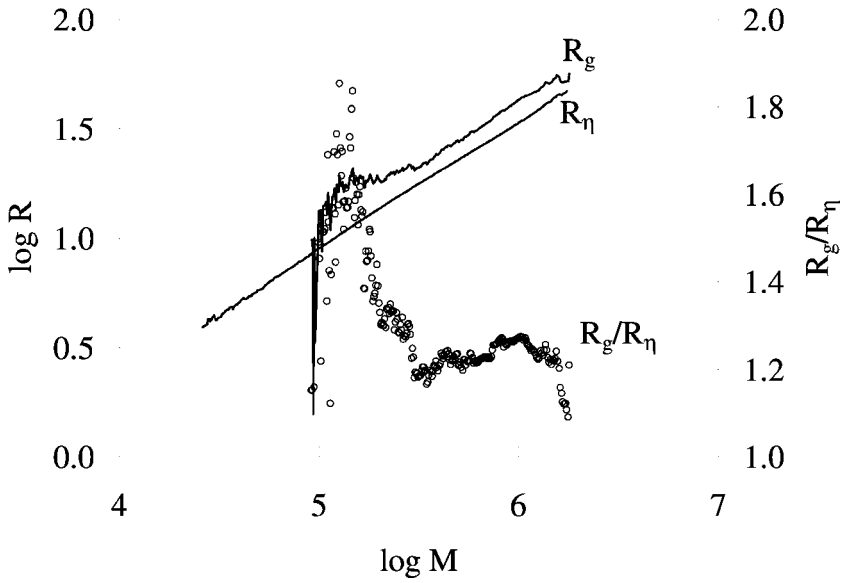

FIGURE 5 Radius of gyration and viscometric radius conformation plots for broad polystyrene, as in Figures 1 and 2. The viscometric radius is calculated from local intrinsic viscosities and molecular weights (via a universal calibration curve) measured by the viscometry detector and Equation (36). Local radius of gyration values are from two-angle light scattering detection. The ratio of radii is plotted on the second y-axis.

reported for polystyrene in good solvents[94]. Note that the accessible molecular weight range is limited by the smallest size measurable by LS detection. In a similar comparison of radii, the ratio R_g/R_η of polystyrene stars in dimethylacetamide showed the expected increase in the viscometric radius compared to linear polystyrene and also exhibited a change in the generalized ratio toward that of linear polymers with ultrasonic degradation[95]. The data suggested that degradation occurred preferentially at the star center, resulting in linear arms.

The basis for quantitating polymer topology by SEC with molecular-weight-sensitive detection involves calculation of the molecular contraction factor, g,

$$g = \left[\frac{R_g^2}{(R_g^2)_L}\right]_M \tag{38}$$

where the comparison is made at equivalent molecular weight (i.e., at vertical slices of $\log M$ versus $\log R_g$ conformation plots obtained from SEC-LS). The method requires a linear analog of the branched molecule. The number of branch points can be estimated from g as a function of M from statistical models for a variety of chain conformations. At small sizes, the radius of gyration may not be measurable, depending on the magnitude of the scattering vector, q. In such instances, a viscometric molecular contraction factor can usually be measured by SEC-viscometry,

$$g' = \left[\frac{[\eta]}{([\eta])_L}\right]_M \tag{39}$$

or from the molecular weight measured by light scattering at equivalent retention volumes using the molecular weight of a linear analog, M_L^*,

$$g' = \left[\left(\frac{M_L^*}{M_{BR}}\right)^{1+a}\right]_{V_r} \tag{40}$$

where a is the Mark-Houwink exponent of the linear polymer[96,97]. Attempts to relate the g' molecular contraction factor to the theoretically better understood g factor suggest that an empirical relation holds,

$$g = g'^{\frac{1}{b}} \tag{41}$$

where b is a function of polymer architecture and solvent draining. Theoretical predictions of b are larger for long-chain branching ($\sim$1.5) than for regular star molecules ($\sim$0.5)[98,99], but experimental and theoretical values of b can differ considerably, depending on solvent and polymer structure[100]. The unique aspect of multidetector SEC is that both the g and g' molecular contraction factors are measured as a function of molecular weight for those regions of the molecular size distribution that are accessible to both light scattering and viscometry detection. Thus, the relationship given by Equation (41) can now be tested with multidetector SEC for a wide variety of polymer topologies in various solvents as a function of molecular weight. In this respect, much literature has appeared in the past three years on several polymer topologies.

Stars

Star polymers are a special case of branching, distinguished by chains radiating from a compact core. This class of branched polymers has been the subject of numerous investigations over the years, and the work is summarized in an excellent recent review[101]. The complexity of SEC

characterization can depend on the method of synthesis. Arms can be analyzed before linking them to a central terminus in "arm-first" preparations, which greatly simplifies the estimation of the number of arms to that of simple molecular weight measurements. The number of arms in even complex structures, such as star-shaped polystyrenes with star-shaped branches at the terminal chain ends prepared "arm first," can be characterized through analysis of the starting arms and completed stars by SEC-LS[102] or SEC-viscometry. Stars made by "core-first" methods that grow arms from a central terminus do not have precursor arms that can be analyzed before assembly to star structures. In such instances, the molecular contraction factor can be used to estimate the number of arms, f_s, from a model such as that of Zimm and Stockmayer[103] for regular stars, which in rearranged form is:

$$f_s = \frac{3 + \sqrt{9 - 8g}}{2g} \tag{42}$$

A solution for stars with f polydisperse arms is[104,105]:

$$g_z = \frac{3f}{(f+1)^2} \tag{43}$$

The molecular contraction factor g is measured directly by multi-angle light scattering detection. The molecular contraction factor g' of small stars is often easier to measure, but a less certain theoretical relationship exists between g' and f_s. There is also enough uncertainty in the exponent b of Equation (41) to introduce a significant error in the calculation of the number of arms; the theoretical value is $b = 0.5$ in a θ solvent, and typical experimental values are $b = 0.79$ for polystyrene stars in tetrahydrofuran[106]. Fortunately, a large amount of data exists from which an empirical relationship has been established between g and g' that appears to be valid for many star polymers in different solvents[93]. More recently, data from the literature were fit to provide a relationship between g' and f for use with SEC with viscometry detection[107]. SEC with molecular-weight-sensitive detection has been used to characterize homopolymer stars of polystyrene[108,109], poly(methyl methacrylate)[110], poly(1,3-cyclohexadiene)[111], and poly(ε-caprolactone)[112]. Two publications presented deconvolution methods for calculating the number of arms in mixtures of star polymers[107,109]. Star-*block*-linear-*block*-star triblock (pom-pom) polystyrenes[113], amide core-functionalized PMMA star polymers[114], tCum[poly(isobutylene-b-norbornadiene]$_3$ and tCum[poly(norbornadiene-b-isobutylene]$_3$ block stars[115], star-shaped polystyrene-*block*-polybutadiene[116], and star polystyrene-*block*-(linear polydimethylsiloxane)-*block*-(star polystyrene)[117] are examples of more

complicated star architectures analyzed by SEC with molecular-weight-sensitive detection. Star-block copolymers such as the last example are more difficult to characterize because of the potential for variation in the specific refractive index increment across the molecular size distribution. This variation affects the calculation of local molecular weight by light scattering and also introduces error in the local concentration, c_i, from the DRI detector. Block copolymers, in general, remain problematic for SEC with molecular-weight-sensitive detection, if the concentration detector response is not constant across the molecular size distribution. Nonlinear block copolymers, such as for combs, centipedes, and barbwires of poly(isoprene-*graft*-styrene) with trifunctional, tetrafunctional, and hexafunctional branch points[118], are even more complicated and may require special methods, such as interaction chromatography used for miktoarm stars[119] and a spectrophotometric detector in addition to light scattering DRI detectors for star-block copolymers[120].

Long-Chain Random Branching

The basis of long-chain branching (LCB) characterization is, again, the measurement of molecular contraction factors that are used with suitable models to estimate the number of long-chain branches as a function of molecular weight. An introduction to the subject appeared recently[121]. The Zimm-Stockmayer model[103] is commonly used for polymers with random trifunctional branching, with number average branch sites B_{3n}:

$$g = \left\{ \left(1 + \frac{B_{3n}}{7} \right)^{\frac{1}{2}} + \frac{4B_{3n}}{9\pi} \right\}^{-\frac{1}{2}} \tag{44}$$

This analysis continues to be a mainstay in low-density polyethylene characterization, and many applications in the past three years involve new polyolefins. For example, LCB SEC-MALLS analysis of metallocene-catalyzed ethylene homopolymers was correlated with ^{13}C NMR (nuclear magnetic resonance) structure characterization and rheology[122]. SEC-MALS was used to provide insight into the mechanism of long-chain branching in isotactic polypropylene synthesized using a metallocene catalyst[123,124]. In one of the few non-polyolefin applications, natural rubbers were examined by SEC-viscometry[125]. Multidetector systems using both light scattering and viscometry detection are capable of elucidating the exponent b of Equation (41) as a function of molecular weight. In one example for low-density polyethylene, b varied in a non-monotonic manner from approximately 0.5 to 1.25 for molecular weights between 10^5 and 10^7[126]. In another low-density polyethylene study, b was approximately constant ($b \sim 1.0$) as a function of molecular

weight[127]. A value of $b = 0.73$ was measured for several polybutadiene and (polyethylene-1-butene) combs[128], which also exhibited g' factors that decreased with increases in branch length, as predicted by a model of Berry-Orofino. In another example, $b = 0.73$ for dextran, independent of molecular weight[129]. The Flory draining factor Φ_i relating intrinsic viscosity, radius of gyration, and molecular weight,

$$[\eta]_i = \Phi_i \frac{R_{g,i}^3}{M_i} \tag{45}$$

estimated from g factors,

$$\Phi_{i,branch} = \Phi_{i,linear} g(M_i)^{b-3/2} \tag{46}$$

was shown to increase with increasing amounts of branching (which increases with molecular weight). The interpretation is that the molecules drain less with increasing amount of branching, which is plausible because the structures are denser.

It is still not clear if the differences observed between b values for randomly branched polymers are a result of different chemical structures or are related to possible systematic errors in multidetector SEC, such as those caused by interdetector volume uncertainty and axial dispersion.

Hyperbranched Polymers and Dendrimers

Hyperbranching is a special case of statistical branching for monomers that have one functional group A that can react only with another functional group B on the same monomer. The reaction is clearly not random, and the molecular weight distributions for A_yB_x are predicted from simple statistics. Dendrimers with branch functionality f are systematically grown in generations leading to Cayley tree structures that increase in the number of monomers successively with each added generation. Both hyperbranched polymers and dendrimers have compact structures in solution compared to linear polymers and long-chain branched materials, and, consequently, they exhibit small molecular contraction factors.

Recent SEC-viscometry detection examples include examination of hyperbranched polyesteramides[130,131], polyalkoxysiloxanes[132], and aliphatic polyesters and their trimethylsilylated derivatives[133]. SEC-LS examples include hyperbranched polyisobutylenes[134], regular polystyrene dendrigrafts[135], poly(ether amide)s[136], commercial aliphatic polyesters based on 2,2-bis(methylol)propionic acid[137], divinylbenzene-ethylstyrene hyperbranch copolymers[138], poly(ε-caprolactone)s having different lengths of homologous backbone segments[139], and acetylated poly(amidoamine) dendrimers[140]. Triple detection examples include hyperbranched poly(methyl methacrylate)s[141], polyurethanes[142],

aromatic polyesters[143,144], poly(acrylic acid)[145], polyacrylates[146], and lactosylated polyamidoamine dendrimers[147]. A partial review of examples from the literature prior to 2001 also appeared recently[148].

An interesting example is the comprehensive study of De Luca and Richards[143] on an aromatic hyperbranched polymer. They used SEC-viscometry with right-angle light scattering detection, which does not measure the radius of gyration directly. They carefully analyzed precipitated fractions by a combination of conventional light scattering, dynamic light scattering, viscometry, and triple-detection SEC. The resulting analysis of generalized radii ratios, fractal dimensions from conformation plots, and unperturbed dimensions was extensive and revealing. Potentially, future analyses will be simplified and improved with an SEC-multidetector combination of viscometry, multi-angle elastic light scattering, and dynamic light scattering, without the need for precipitated fractions.

Perfectly grown dendrimers are monodisperse in molecular weight, and the advantage of SEC molecular-weight-sensitive detection becomes less significant than with broad distribution materials. In contrast, the molecular weight distributions of hyperbranched polymers can be quite broad, and the number molecular weight distribution is predicted to follow a power law with an exponential cutoff with a characteristic molecular weight M_{char}:

$$\phi(M) = M^{-\tau} e^{(-M/M_{char})} \tag{47}$$

with $\tau = 1.5$ and $M_{char} = \varepsilon^{-2}$, where $\varepsilon = (f-1)p - 1$ is the relative extent of reaction at high degrees of polymerization for p fraction of B groups reacted[9]. The predictions can be tested by converting the experimental weight fraction molecular weight distribution obtained by SEC-viscometry of SEC-LS to the number distribution,

$$\phi(M) = \frac{N_A W_n(\log M)}{\ln(10) M^2} \tag{48}$$

The example shown in Figure 6, calculated from data for aromatic hyperbranched polymers with different extents of reaction[144], has a power law dependence with $\tau \sim 2.2$. This is a significant departure from the mean-field prediction of $\tau \sim 1.5$ for hyperbranched polymers, and it is also the well-known percolation model value for random branching. In addition, the statistics used to derive Equation (47) have important predictions for the whole polymer molecular weight averages. The number-average molecular weight prediction is $M_n \sim \varepsilon^{-1}$ and all higher averages $M_w \sim M_z \sim M_{z+1} \sim \varepsilon^{-2}$. In other words, the polydispersity ratio

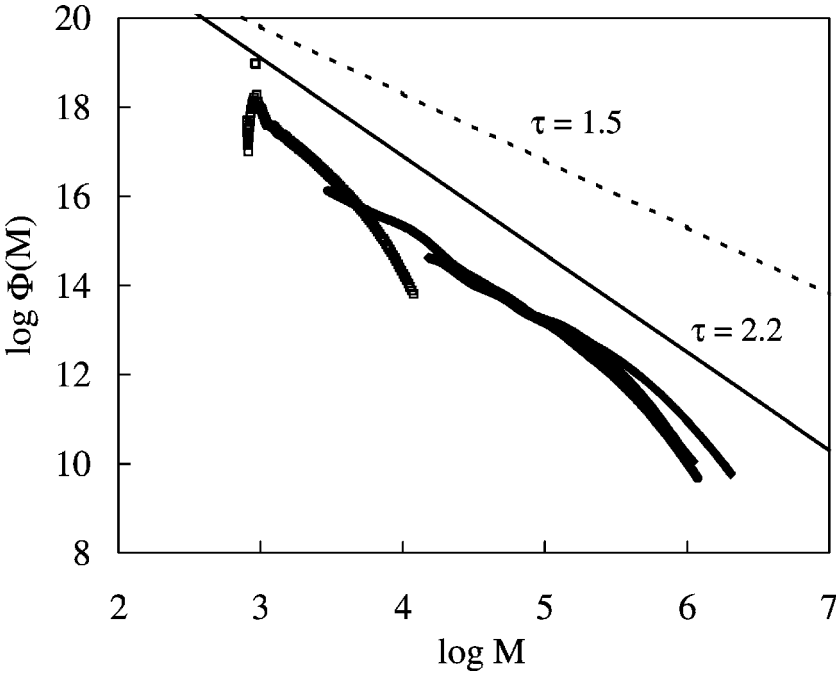

FIGURE 6 Number distribution for three aromatic hyperbranched polymers at different extents of reaction, from Yamaguchi et al.[144] Solid lines are visual aides offset from the actual data, showing predictions for Equation (47) with $\tau = 1.5$ and $\tau = 2.2$.

M_w/M_n diverges as M_n with extent of reaction and the polydispersity ratios M_z/M_w, M_{z+1}/M_z, etc., converge to a constant value. The polydispersity ratios of the samples shown in Figure 6 were more consistent with random branching than hyperbranching. Geladé et al.[131] arrived at a similar conclusion of random branch structure on hyperbranched polyesteramides from the fractal dimensions obtained from SEC-viscometry conformation plots and from small-angle neutron scattering. Other wrokers have reported $\tau \sim 1.5$ for hyperbranched polyesters from plots rescaled with respect to M_w, which collapses all of the number distributions for a family of hyperbranched polymers with different molecular weight distributions on a universal curve[149,150]. The statistical predictions for hyperbranched ploymers assume equal reactivity of B groups and no intramolecular reactions–assumptions that are never really true for hyperbranching chemistry. Examination of the molecular weight number distributions and polydispersity indices measured by SEC with

molecular-weight-sensitive detection, thus, provides some proof (or lack of) pure hyperbranch topology and is an excellent complement to NMR and mass spectrometry (MS) structure characterization of these materials.

Physiochemical Studies

A common application of SEC with molecular-weight-sensitive detection is the study of phase separation. Recent examples include the use of light scattering detection in the molecular weight fractionation of chitin in N,N-dimethylacetamide/lithium chloride[151], fractionation of lignosulfonates in ethanol-water[152,153], and phase-separation-induced fractionation in aqueous gelatin and dextran mixtures[154]. Related is the isolation of components by extraction or solvent-nonsolvent fractionation, such as extraction of water soluble β-glucan fractions from milled seeds of oat cultivar[155], extraction of polysaccharide-protein complexes from *Ganoderma tsugae* mycelium[156], and fractionation of polysaccharides from sclerotia of *Pleurotus tuber-regium*[157]. In such studies, light scattering is used primarily as a means to measure the molecular weight distributions and radii of gyration of fractions.

Light scattering detection is ideal for studies involving association and aggregation when very large molecules are formed. Examples include: the association of polyurethanes in polar solvents[158] and lignins in N,N-dimethylformamide[159]; self-aggregation of gelatin above the gelation temperature[160]; the formation of stable aggregates in solutions of ethyl(hydroxyethyl)cellulose[161]; the gradual dissolution of clusters in dilute solutions of poly(dimethylcarbosiloxane) with carboxylic acid groups and hydrophobically modified polyacrylamide and its charged terpolymer[162]; soluble aggregates from whey protein isolate[163]; reduced lactose whey dispersions[164] and commercial whey protein products[165]; aggregates of human immunoglobin G[166]; aggregation of proteins induced by high shear rates[167]; configurations of high-molecular-weight species in pertussis vaccine components[168]; and self-association of soluble proteins such as FliJ[169]. A more complicated case is the determination of the association state of conjugated proteins. A UV detector used at a wavelength for proteins is combined with refractive index and light scattering detectors in a "three-detector method" originally developed in the laboratories of Takagi[170] and Arakawa[171]. Improvements in the calibration procedures for the three detectors were recently presented[172]. A recent application used the three-detector method to determine trimeric subunit stoichiometry of glutamate transporters[173]. Transitions of *lentinan* from coil to triple helix[174] and from coil to double helix transitions of ι-carrageenan as a function of the amount of υ-carrageenan monomer units[175] are other examples where the formation

of large, high-molecular-weight species as a function of solvent conditions can be detected easily by light scattering detection. Also, light scattering detection is very sensitive to aggregates and undissolved materials in solution, including kraft pulp celluloses in lithium chloride/N,N-dimethylacetamide (DMAc)[176], hydroxypropyl celluloses in aqueous sodium chloride[79], hyaluronic acids in phosphate buffer solutions[177], and self-assembling copolymers derived from α, β-poly(N-2-hydroxyethyl)-DL-aspartamide[178] in aqueous solution and DMAc.

Gelation is a final application of molecular-weight-sensitive detection for studying the evolution of high-molecular-weight species. The number distribution Equation (47) has been used to demonstrate that randomly branched melt condensation polyesters belong to the critical percolation universality class for small lengths between branch points and to the mean-field class that is modeled by the Flory-Stockmayer theory for branched polyesters with long linear chains between branch points[179,60]. Recent gelation studies include estimating the average functionality of cross-linked 3,4-dihydroxyphenylalanine-modified poly(ethylene glycols)[180] and estimating the gel point in copolymerizations of allyl methacrylates with several alkyl methacrylates[181].

Miscellaneous

Although the responses for viscometry and light scattering detectors diminish with decreasing molecular weight, in some instances both detectors have sufficient sensitivity to study low-molecular-weight polymers. Both detectors are commonly used to study polymer degradation. A recent example is the use of SEC-MALS in characterization and modeling of the hydrolysis of polyamide-11[182]. In some instances, oligomers and small molecules can be studied. For example, Xie et al. examined the applicability of MALS to the analysis of oilgomers[183], and Podzimek used MALS to determine molecular weight distributions of oligomeric epoxy resins[184]. Striegel ascertained the degree of polymerization of styrene oligomers at which the intrinsic viscosity in dimethylacetamide/lithium chloride changed from positive to negative[185] and ruled out the possibility of analyte clustering by light scattering detection.

An adaptation of SEC-LS detection is the study of polymer optical anisotropy as a function of molecular weight. Striegel used a MALS instrument fitted with horizontal and vertical polarizers between the flow cell and the photodiode detectors[186,187] to measure a depolarization ratio of the horizontally and vertically polarized scattering intensities. Depolarization was observed in the low-molecular-weight regions of isotactic PMMA and brominated polystyrene. However, optical anisotropy was not observed, as expected for helical, rigid poly(benzyl

glutamate), with possible explanations offered such as complications arising from alignment of molecules in the flow cell, solvent refractive index, observation angle, and concentration dependencies.

Another adaptation of multi-angle light scattering detection is the estimation of second virial coefficients. In one example, A_2 was estimated from Zimm plots constructed from a series of injections of ι-carrageenan at different concentrations[188]. The second virial coefficient changed from positive to negative with decreasing molecular weight. The concentration range that can be examined by the technique may be limited by concentration dependencies on the size-exclusion fractionation itself, and, as presented, this method had not been rigorously evaluated. Others are using SEC-LS for estimation of A_2 by injecting a concentration series of samples, apparently with reasonable correlation to independent measurements[92], although few experimental details have been presented.

Another method for estimating the second virial coefficient of monodisperse proteins or unfractionated polydisperse materials injected into an SEC-MALS was patented by Wyatt[189]. The method requires that the molecular weight, M, of the material is known. Combined with the sum of extrapolated zero-angle excess Rayleigh scattering intensities, $R(0^\circ)$, of a peak eluted from an SEC column, the total mass injected, m_t, and the sum of concentrations, c_i, obtained from a DRI or other concentration detector, the second virial coefficient is estimated from:

$$A_2 = \frac{Mm_t - \sum_i R(0^0)/K}{2M^2 \sum_i c_i^2} \tag{49}$$

The patent also suggests a method for determining solvent conditions when $A_2 = 0$, although no examples are given. A method for proteins that uses the SEC retention volumes and average concentrations of a concentration series, without a light scattering detector, may also be of interest to those attempting to measure second virial coefficients[190].

SUMMARY

The number of applications of SEC with molecular-weight-sensitive detection continues to increase compared to previous years, although the number of literature citations still represents less than 4% of the total number of publications involving some form of size exclusion. Many new users have appeared in the literature over the past three years, crossing multiple disciplines and studying diverse materials. The applications are extending far beyond simple molecular weight measurements,

demonstrated by the examples chosen for this review. The interrelationships between absolute molecular weight, radius of gyration, viscometric and hydrodynamic radii are able to define macromolecular conformation, structure, and behavior in dilute solution as never before. Also, the once amusing debates over the advantages of light scattering versus viscometry detection are less common. In fact, the trend continues toward multidetection that includes both viscometry and light scattering (now elastic and inelastic), as vendors that once exclusively manufactured light scattering instruments are now introducing complementary viscometers, and vice versa. The advantages of on-line dilute solution characterization of large molecules by SEC with molecular-weight-sensitive detection has become more obvious to many workers; still, there remains a large percentage of SEC users that have not yet invested in the technology. Continued improvements in the hardware and software of integrated multidetector systems may attract new users. More likely, the ever-increasing complexity of macromolecular structures generated by new synthetic methods and the continued elucidation of complex biomacromolecular structure will create characterization challenges that necessitate their use.

NOMENCLATURE

a	Mark-Houwink exponent
b	scaling exponent for $g - g'$ power law
$A_{2,i}$	second virial coefficient at elution point i
B_{3n}	number-average number of branch sites in a trifunctional, randomly branched polymer molecule
c_i	concentration at elution point i
d_f	fractal dimension
D_2	slope of $\ln M$ vs. retention volume calibration curve
$D_{2\eta}$	slope of $\ln[\eta]$ vs. retention volume calibration curve
$(dn/dc)_i$	specific refractive index increment at elution point i
f	branch site functionality
f_s	number of arms in a regular star molecule
g	radius of gyration molecular contraction factor
g'	intrinsic viscosity molecular contraction factor
g_{SCB}	short-chain branching radius of gyration molecular contraction factor
g'_{SCB}	short-chain branching intrinsic viscosity molecular contraction factor
i	data point at a given elution volume
I	detector signal intensity

J_i	hydrodynamic volume at elution point i
J_i^*	reconstructed hydrodynamic volume at elution point i
K_a	intrinsic viscosity – molecular weight scaling prefactor
K_i	light scattering optical constant at elution point i
K_v	radius of gyration – molecular weight scaling prefactor
l	length of viscometry detector capillary
LS_i	light scattering detector signal
m_t	mass of sample injected
M_{char}	characteristic molecular weight
M_L^*	molecular weight of linear polymer at same elution volume of a branched polymer
M_{BR}	molecular weight of branched polymer
M_i	molecular weight at elution point i
M_n	whole polymer number-average molecular weight
$M_{n,i}$	number-average molecular weight at elution point i
M_q	whole polymer qth molecular weight average
M_w	whole polymer weight-average molecular weight
$M_{w,i}$	weight-average molecular weight at elution point i
$M_{i,c}$	molecular weight at elution point i corrected for axial dispersion
$M_{i,uc}$	molecular weight at elution point i uncorrected for axial dispersion
M_z	whole polymer Z-average molecular weight
n	solvent refractive index
N_A	Avogardro's number
p	extent of reaction
ΔP	pressure drop across a viscometry detector capillary
P_i	pressure drop of sample solution across a viscometry detector capillary
P_{in}	inlet pressure of a differential viscometry detector
P_0	pressure drop of solvent across a viscometry detector capillary
P_{diff}	differential pressure of a differential viscometry detector
$P(\theta)_i$	particle scattering function at elution point i
$P(\theta_1)_i$	particle scattering function at angle 1 at elution point i
$P(\theta_2)_i$	particle scattering function at angle 2 at elution point i
q	scattering vector
Q	flow rate
r	radius of viscometry detector capillary
$R(\theta)_i$	excess Rayleigh scattering at elution point i
$R(0^0)$	zero angle excess Rayleigh scattering
$R(\theta_1)_i$	excess Rayleigh scattering at angle 1 at elution point i
$R(\theta_2)_i$	excess Rayleigh scattering at angle 2 at elution point i
$R_{g,i}$	radius of gyration at elution point i
$(R_g)_L$	radius of gyration of a linear polymer

R_h	hydrodynamic radius
R_η	viscometric radius
R_T	thermal radius
Δv_i	volume increment between data points
V	retention volume
W_i	concentration chromatogram height at elution point i
W_{i}^*	reconstructed concentration chromatogram height at elution point i
$W_{N,i}$	normalized concentration chromatogram height at elution point i
$W_{N,i}$ (log[η])	intrinsic viscosity distribution weight fraction
Z_i	dissymmetry at elution point i

Greek letters

α	light scattering optical constant not containing dn/dc
β	DRI response constant
ε	relative extent of reaction
γ	exponent relating detector signal intensity and molecular weight
λ_0	wavelength of light in vacuum
η	viscosity measured by pressure drop in viscometry detector capillary
η_i	viscosity of sample solution measured by viscometry detector capillary at elution point i
η_0	solvent viscosity
$\eta_{sp,i}$	specific viscosity at elution point i
$\eta_{red,i}$	reduced viscosity at elution point i
$[\eta]$	whole polymer intrinsic viscosity
$[\eta]_i$	intrinsic viscosity at elution point i
$[\eta]_{i,c}$	intrinsic viscosity at elution point i corrected for axial dispersion
$[\eta]_{i,uc}$	intrinsic viscosity at elution point i uncorrected for axial dispersion
$[\eta]_i^*$	intrinsic viscosity at elution point i corrected for finite concentration
$[\eta]_L$	intrinsic viscosity of a linear polymer
θ	angle of scattered light relative to incident beam
σ	standard deviation band spreading parameter
$\phi(M)$	number of molecules with molecular weight M
Φ	Flory draining parameter
ξ	$(2a-1)/3$
τ	exponent of number distribution – molecular weight scaling relationship
υ	radius of gyration – molecular weight scaling exponent

REFERENCES

[1] Ouano, A. C. (1972) *J. Polym. Sci. Part A-1*, **10**, 2169.
[2] Ouano, A. C. and W. Kaye. (1974) *J. Appl. Polym. Sci.* **12**, 1151.
[3] Yau, W. W. (1991) *J. Appl. Polym. Sci.*, **48**, 85.
[4] Lehmann, U., W. Köhler, and W. Albrecht. (1996) *Macromolecules*, **29**, 3212.
[5] Podzimek, S. (2002) *Amer. Lab.*, **34**, 38, 40–42, 45.
[6] Jumel, K. (2002) In *Carbohydrate Analysis by Modern Chromatography and Electrophoresis*, ed. Ziad El Rassi, p. 341. Amsterdam: Elsevier.
[7] Mendichi, R. and A. G. Schieroni. (2001) *Curr. Trends in Polym. Sci.* **6**, 17.
[8] Teraoka, I. (2002) *Polymer Solutions*. New York: John Wiley.
[9] Rubinstein, M. and R. H. Colby. (2003) *Polymer Physics*. New York: Oxford University Press.
[10] Cazes, J., ed. (2001) *Encyclopedia of Chromatography*, New York: Marcel Dekker.
[11] Jackson, C. and H. G. Barth. (1995) *Chromatogr. Sci. Ser.*, **69**, 103.
[12] Yau, W. W. (1990) *Chemtracts Macromol. Chem.*, **1**, 1.
[13] Lecacheaux, D., J. Lesec, and C. Quivoron. (1982) *J. Appl. Polym. Sci.*, **27**, 4867.
[14] Yau, W. W., S. D. Abbott, G. A. Smith, and M. Y. Keating. (1987) In *Detection and Data Analysis in Size Exclusion Chromatography*, ed. T. Provder, p. 80. Washington, D.C.: American Chemical Society.
[15] Haney, M. A. (1985) *J. Appl. Polym. Sci.*, **30**, 3037.
[16] Lesec, J. (2001) In *Encyclopedia of Chromatography*, ed. J. Cazes p. 872. New York: Marcel Dekker.
[17] Norwood, D. P. and W. F. Reed. (1997) *Int. J. Polym. Anal. Charact.*, **4**, 99.
[18] Brun, Y. (2001) In *Encyclopedia of Chromatography*, ed. J. Cazes, p. 441. New York: Marcel Dekker.
[19] Kirkland, J. J., S. W. Rementer, and W. W. Yau. (1991) *J. Appl. Polym. Sci. Appl. Polym. Symp.*, **48**, 39.
[20] Hamielec, A. E. and A. C. Ouano. (1978). *J. Liq. Chromatogr.*, **1**, 111.
[21] Goldwasser, J. M. (1993) In *Chromatography of Polymers: Characterization by SEC and FFF*, ed. T. Provder, p. 243. Washington, D.C.: American Chemical Society.
[22] Goldwasser, J. M. (1989) In *Proceedings of the International Gel Permeation Symposium*, *Newton*, Mass., p. 150.
[23] Huang, Y., Z. Xu, Y. Huang, D. Ma, J. Yang, and J. W. Mays. (2003) *Int. J. Polym. Anal. Char.*, **8**, 383.
[24] Haney, M. A., Honey, M. A., C. Jackson, and W. W. Yau. (1991) In *Proceedings of the International Gel Permeation Symposium*, *San Francisco*, p. 49.
[25] Wyatt, P. J., D. L. Hicks, C. Jackson, and G. K. Wyatt. (1988) *Am. Lab.*, **20**, 108, 110, 112–113.
[26] Zimm, B. H. (1948) *J. Chem. Phys.*, **16**, 1099.
[27] Berry, G. C. and P. M. Cotts, (1999) Static and dynamic light scattering, in *Experimental Methods in Polymer Characterization*, eds. R. A. Pethnick, and R. S. Stein, p. 1. New York: John Wiley.
[28] Andersson, M., B. Wittgren, and K.-G. Wahlund. (2003) *Anal. Chem.*, **75**, 4279.
[29] Frank, R., L. Frank, and N. Ford. (1995) In *Chromatographic Characterization of Polymers: Hyphenated and Multidimensional Techniques*, eds. T. Provder, H. Barth, and M. W. Urban, p. 109. Washington, D.C.: American Chemical Society.

[30] Mourey, T. H. and H. Coll. (1995) In *Chromatographic Characterization of Polymers: Hyphenated and Multidimensional Techniques*, eds. T. Provder, H. Barth, and M. W. Urban, p. 123. Washington, D.C.: American Chemical Society.
[31] Cassassa, E. F. (1999) Particle scattering factors in Rayleigh scattering, in *Polymer Handbook*, eds. J. Brandup, E. H. Immergut, and E. A. Grulke, V 3rd edition, section VII, p. 629. New York: John Wiley.
[32] Mourey, T. H. and H. Coll. (1995). *J. Appl. Polym. Sci.*, **56**, 65.
[33] Wyatt, P. J. and R. Myers. (2001) In *Encyclopedia of Chromatography*, ed. J. Cazes, p. 384. New York: Marcel Dekker.
[34] Bartlett, T. and T. Havard. (2001) In *GPC Symposium Proceedings 2000*. Milford, Mass.: Waters Corporation.
[35] Trainhoff, S. (2001) In *GPC Symposium Proceedings 2000*. Milford, Mass.: Waters Corporation.
[36] Jones, W. R. (2002) *Amer. Biol. Lab.* **20**, 36.
[37] Cotts, P. M. (2003) In *Abstracts of Papers, 225th ACS National Meeting, New Orleans, March 23–27*.
[38] Liu, Y., B. Shuqin, Y. Zhu, and W. Zhang. (2003) *Polymer*, **44**, 7209.
[39] Brun, Y., M. V. Gorenstein, and N. Hay. (2000) *J. Liq. Chromatog. & Relat. Technol.*, **23**, 2615.
[40] Lew, R., P. Cheung, S. T. Balke, and T. H. Mourey. (1993) *J. Appl. Polym. Sci.*, **47**, 1685.
[41] Yau, W. W. and D. Gillespie. (2002) *Polymer*, **42**, 8947.
[42] Hamielec, A. E. (1980) *J. Liq. Chromatogr.*, **3**, 381.
[43] Jackson, C. and W. W. Yau. (1993) *J. Chromatogr.*, **645**, 209.
[44] Netopilík, M., S. Podzimek, and P. Kratochvil. (2001). *J. Chromatogr. A*, **922**, 25.
[45] Netopilík, M. (2001) *Int. J. Polym. Anal. Charact.*, **6**, 349.
[46] Netopilík, M. (2003) *J. Biochem. Biophys. Methods*, **56**, 79.
[47] Wittgren, B., A. Welinder, and B. Porsch. (2003) *J. Chromatogr. A*, **1002**, 101.
[48] Podzimek, S., T. Vlcek, and C. Johann. (2001) *J. Appl. Polym. Sci.*, **81**, 1588.
[49] Teresa, M., R. Laguna, R. Medrano, M. P. Plana, and M. P. Tarazona. (2001) *J. Chromatogr. A*, **919**, 13.
[50] Mendichi, R. and A. G. Schieroni. (2002) *Polymer*, **43**, 6115.
[51] Parth, M., N. Aust, and K. Lederer. (2003) *Int. J. Polym. Anal. Charact.*, **8**, 175.
[52] Aust, N., M. Parth, and K. Lederer. (2001). *Int. J. Polym. Anal. Charact.*, **6**, 245.
[53] Balke, S. T. and T. H. Mourey. (2001) *J. Appl. Polym. Sci.*, **81**, 370.
[54] Brun, Y. (1998) *J. Liq. Chromatogr. Relat. Technol.*, **21**, 1979.
[55] Medrano, R., M. T. R. Laguna, E. Saiz, and M. P. Tarazona. (2003). *Phys. Chem. Chem. Phys.*, **5**, 151.
[56] Schlaad, H. and P. Kilz. (2003) *Anal. Chem.*, **75**, 1548.
[57] Drott, E. E. (1977) *J. Chromatogr. Sci.*, **8**, 41.
[58] Mourey, T. H. and T. G. Bryan. (2002) *J. Chromatogr. A*, **964**, 169.
[59] Chen, J., W. Radke, and H. Pasch. (2003) *Macromol. Symp.*, **193**, 107.
[60] Lusignan, C. P., T. H. Mourey, J. C. Wilson, and R. H. Colby. (1999) *Phys. Rev. E.*, **60**, 5657.
[61] Zhang, L., M. Zhang, J. Guo, Y. Song, and P. C. Cheung. (2001) *Biopolymers*, **59**, 457.
[62] Ding, Q., L. Zhang, X. Xu, X. Zhang, and C. Wu. (2001) *J. Macromol. Sci. Phys.*, **B40**(2), 147.

[63] Kato, H., Y. Sasanuma, A. Kaito, N. Tanigaki, Y. Tanabe, and S. Kinugasa. (2001) *Macromolecules*, **34**, 262.
[64] Radosta, S., M. Haberer, and W. Vorweg. (2001) *Biomacromolecules*, **2**, 970.
[65] Carceller, J.-L. and T. Aussenac. (2001) *J. Cereal Sci.*, **33**, 131.
[66] Mendichi, R., V. Rizzo, M. Gigli, and A. G. Schieroni. (2002) *Bioconjugate Chem.*, **13**, 1253.
[67] Lee, K. Y., K. H. Bouhadir, and D. J. Mooney. (2002) *Biomacromolecules*, **3**, 1129.
[68] Sanchez, C., D. Renard, P. Robert, C. Schmitt, and J. Lefebvre. (2002) *Food Hydrocoll.*, **16**, 257.
[69] Yoo, S.-H. and J.-L. Jane. (2002) *Carbohydr. Polym.*, **49**, 307.
[70] Teresa, M., R. Laguna, J. Gellego, F. Mendicuti, E. Saiz, and M. P. Tarazona. (2002) *Macromolecules*, **35**, 7782.
[71] Schult, T., T. Hjerde, O. I. Optun, P. J. Kleppe, and S. Moe. (2002) *Cellulose*, **9**, 149.
[72] Hwang, H. J., S. W. Kim, C. P. Xu, J. W. Choi, and J. W. Yun. (2002) *J. Appl. Microbiol.*, **94**, 708.
[73] Hwang, H.-J., S.-W. Kim, and J.-W. Choi. (2003) *Enzyme Microbiol. Technol.*, **33**, 309.
[74] Hokputsa, S., K. Jumel, C. Alexander, and S. E. Harding. (2002) *Carbohydr. Polym.*, **52**, 111.
[75] Šoltés, L. and R. Mendichi. (2003) *Biomed. Chromatogr.*, **17**, 376.
[76] Hokputsa, S., C. Hu, B. S. Paulsen, and S. E. Harding. (2003) *Carbohydr. Polym.*, **54**, 27.
[77] Peng, Y., L. Zhang, F. Zeng, and Y. Xu. (2003) *Carbohydr. Polym.*, **54**, 297.
[78] Pfefferkorn, P., J. Beister, A. Hild, H. Thielking, and W.-M. Kulicke. (2002) *Cellulose*, **10**, 27.
[79] Wittgren, B. and B. Porsch. (2003) *Carbohydr. Polym.*, **49**, 457.
[80] Peng, Yanfei, and Lina Zhang. (2003) *J. Biochem. Biophys. Methods*, **56**, 243.
[81] Rolland-Sabaté, A., N.'G. G. Amani, D. Dufour, S. Guilois, and P. Colonna. (2003) *J. Sci. Food Agric.*, **83**, 927.
[82] Meyer, M. and B. Morgenstern. (2003) *Biomacromolecules*, **4**, 1727.
[83] Zhang, M., L. Zhang, and P. C. K. Cheung. (2003) *Biopolymers*, **68**, 150.
[84] Tarazona, M. P. and E. Saiz. (2003) *J. Biochem. Biophys. Methods*, **56**, 95.
[85] Teresa, M., R. Laguna, M. P. Tarazona, and E. Saiz. (2003) *J. Chem. Phys.*, **119**, 1148.
[86] Temyanko, E., P. S. Russo, and H. Ricks. (2001) *Macromolecules*, **34**, 582.
[87] Brugnerotto, J., J. Desbrières, G. Roberts, and M. Rinaudo. (2001) *Polymer*, **42**, 9921.
[88] Fee, M., N. Errington, K. Jumel, L. Illum, A. Smith, and S. Harding. (2003) *Eur. Biophys. J.*, **32**, 457.
[89] Zhang, Lina, Xufeng Zhang, Qi Zhou, Pingyi Zhang, Mei Zhang, and Xuelian Li. (2001) *Polym. Int.*, **33**, 324.
[90] Mendichi, R., L. Šoltés, and A. G. Schieroni. (2003) *Biomacromolecules*, **4**, 1805.
[91] Villegas, J. A., R. Olayo, and J. Cervantes. (2003) *J. Inorg. Organometallic Polym.*, **13**, 205.
[92] Sun, T., P. Brant, R. C. Chance, and W. W. Graessely. (2001) *Macromolecules*, **34**, 6812.
[93] Burchard, W. (1999) In *Branched Polymers II*, ed. J. Roovers, pp. 113–194. Berlin: Springer-Verlag.

[94] Davidson, N. S., L. J. Fetters, W. G. Funk, N. Hadjichristidis, and W. W. Graessley. (1987) *Macromolecules*, **20**, 2614.
[95] Striegel, A. M. (2003) *J. Biochem. Biophys. Methods*, **56**, 117.
[96] Bugada, D. C. and A. Rudin. (1987) *Eur. Polym. J.*, **23**, 847.
[97] Tackx, P. and J. C. J. F. Tacx. (1998) *Polymer*, **39**, 3109.
[98] Zimm, B. H. and R. W. Kilb. (1959) *J. Polym. Sci.*, **37**, 19.
[99] Kurata, M. and M. Fukatsu. (1964) *J. Chem. Phys.*, **41**, 2934.
[100] Mays, J. W. and N. Hadjichristidis. (1992) *J. Appl. Polym. Sci. Appl. Polym. Symp.*, **51**, 55.
[101] Grest, G. S., L. J. Fetters, J. S. Huang, and D. Richter. (1996) In *Star Polymers: Experiment, Theory, and Simulation*, eds. L. Prigogine, and S. A. Rice, pp. 67–163. New York: John Wiley.
[102] Knauss, D. M. and T. Huang. (2003) *Macromolecules*, **36**, 6036.
[103] Zimm, B. H. and W. H. Stockmayer. (1949) *J. Chem. Phys.*, **17**, 1301.
[104] Burchard, W. (1983) *Adv. Polym. Sci.*, **48**, 1.
[105] Burchard, W. (1977) *Marcromolecules*, **10**, 919.
[106] Jackson, C., D. J. Frater, J. W. Mays. (1995) *J. Polym. Sci. Part B Polym. Phys.*, **33**, 2159.
[107] Balke, S. T., T. H. Mourey, D. R. Robello, T. A. Davis, A. Kraus, and K. Skonieczny. (2002) *J. Appl. Polym. Sci.*, **85**, 552.
[108] Robello, D. R., A. Andre, T. A. McCovick, A. Kraus, and T. H. Mourey. (2002) *Macromolecules*, **35**, 9334.
[109] Kaivez, A., X. A. Gallez, D. Doaust, J. Devaux, and P. Godard. (2002) *Polymer*, **43**, 3181.
[110] Hatada, K., T. Kitayama, N. Fujimoto, T. Fukuoka, O. Nakagawa, and T. Nishiura. (2002) *J. Macromol. Sci. Pure Appl. Chem.*, **A39**, 801.
[111] Williamson, D. T., J. F. Elman, P. H. Madison, A. J. Pasquale, and T. E. Long. (2001) *Macromolecules*, **34**, 2108.
[112] Sanda, F., H. Sanada, Y. Shibasaki, and T. Endo. (2002) *Macromolecules*, **35**, 680.
[113] Knauss, D. M. and T. Huang. (2002) *Macromolecules*, **35**, 2055.
[114] Baek, K.-Y., M. Kamigaito, and M. Sawamoto. (2001) *Macromolecules*, **34**, 7629.
[115] Peetz, R. M., A. F. Moustafa, and J. P. Kennedy. (2003) *J. Polym. Sci. Part A Polym. Chem.*, **41**, 740.
[116] Chang, C.-S. and R. C.-C. Tsiang. (2001) *Int. J. Polym. Anal. Charact.*, **6**, 581.
[117] Huang, T. and D. M. Knauss. (2002) *Polym. Bull.*, **49**, 143.
[118] Uhrig, D. and J. W. Mays. (2002) *Macromolecules*, **35**, 7182.
[119] Park, S., D. Cho, K. Im, T. Chang, D. Uhrig, and J. W. Mays. (2003) *Macromolecules*, **36**, 5834.
[120] Se, K., T. Sakakibara, and E. Ogawa. (2002) *Polymer*, **43**, 5447.
[121] Striegel, A. (2001) In *Encyclopedia of Chromatography*, ed. J. Cazes, p. 497. New York: Marcel Dekker.
[122] Gabriel, C., E. Kokko, B. Löfgren, J. Seppälä, and H. Münstedt. (2002) *Polymer*, **43**, 6383.
[123] Weng, W., W. Hu, A. H. Dekmezian, C. J. Ruff. (2002) *Macromolecules*, **35**, 3838.
[124] Agarwal, P. K., R. H. Somani, W. Weng, A. Mehta, L. Yang, L. Liu, and B. S. Hsiao. (2003) *Macromolecules*, **36**, 5226.
[125] Parth, M., N. Aust, and K. Lederer. (2002) *Macromol. Symp.*, **181**, 447.
[126] Beer, F., G. Capaccio, and L. J. Rose. (2001) *J. Appl. Polym. Sci.*, **80**, 2815.
[127] Cotts, P. M. (2002) *Polym. Preprints*, **43**, 297.

[128] Fernyhough, C. M., R. N. Young, D. Poche, A. W. Degroot, and F. Bosscher. (2001) *Macromolecules*, **34**, 7034.
[129] Ioan, C. E., T. Aberle, and W. Burchard. (2001) *Macromolecules*, **34**, 3765.
[130] Van Benthem, R. A. T. M., N. Meijerink, E. T. F. Geladé, C. G. De Koster, Do Dirk Muscat, P. E. Froehling, P. H. M. Hendriks, C. J. A. A. Vermeulen, and T. J. G. Zwartkruis. (2001) *Macromolecules*, **34**, 3559.
[131] Geladé, E. T. F., B. Goderis, C. G. De Koster, N. Meijerink, and R. A. T. M. Van Benthem. (2001) *Macromolecules*, **34**, 3552.
[132] Jaumann, M., E. A. Rebrov, V. Kazakova, A. M. Muzafarov, W. A. Goedel, and M. Möller. (2003) *Macromol. Chem. Phys.*, **204**, 1014.
[133] Garamszegi, L., T. Q. Nguyen, C. J. G. Plummer, and J.-A. E. Månson. (2003) *J. Chromatogr. Relat. Technol.*, **26**, 207.
[134] Paulo, C. and J. E. Puskas. (2001) *Macromolecules*, **34**, 734.
[135] Muchter, Z., M. Schappacher, and A. Deffieux. (2001) *Macromolecules*, **34**, 7595.
[136] Lederer, A., D. Voigt, C. Clausnitzer, and B. Voigt. (2002) *J. Chromatogr. A*, **976**, 171.
[137] Žagar, E. and M. Žigon. (2002) *Macromolecules*, **35**, 9913.
[138] Sato, T., N. Sato, M. Seno, and T. Hirano. (2003) *J. Polym. Sci. Part A Polym. Chem.*, **41**, 3038.
[139] Choi, J. and S.-Y. Kwak. (2003) *Macromolecules*, **36**, 8630.
[140] Majoros, I. J., B. Keszler, S. Woehler, T. Bull, and J. R. Baker, Jr. (2003) *Macromolecules*, **36**, 5526.
[141] Simon, P. F. W. and A. H. E. Müller. (2001) *Macromolecules*, **34**, 6206.
[142] Hong, L., X. Wang. and X. Tang. (2002) *J. Appl. Polym. Sci.*, **85**, 2445.
[143] De Luca, E. and R. W. Richards. (2003) *J. Polym. Sci. Part B Polym. Phys.*, **41**, 1339.
[144] Yamaguchi, N., J.-S. Wang, J. M. Hewitt, W. C. Lenhart, and T. H. Mourey. (2002) *J. Polym. Sci. Part A Polym. Chem.*, **40**, 2855.
[145] Mori, H., D. C. Seng, H. Lechner, M. Zhang, and A. H. E. Müller. (2002) *Macromolecules*, **35**, 9270.
[146] Hong, C.-Y., Y.-F. Zou, and C.-Y. Pan. (2003) *Polym. Int.*, **52**, 257.
[147] Pavlov, G. M., N. Errington, S. E. Harding, and R. R. Korneeva. (2001) *Polymer*, **42**, 3671.
[148] Vladimirov, N. (2001) In *Encyclopedia of Chromatography*, ed. J. Cazes, p. 218. New York: Marcel Dekker.
[149] Suneel, D. M. A. Buzza, D. J. Groves, T. C. B. McLeish, D. Parker, A. J. Keeney, and W. J. Feast. (2002) *Macromolecules*, **35**, 9605.
[150] Kunamaneni, S., D. M. A. Buzza, D. Parker, and W. J. Feast. (2003) *J. Mater. Sci.*, **13**, 2749.
[151] Poirer, M. and G. Charlet. (2002) *Carbohydr. Polym.*, **50**, 363.
[152] Fredheim, G. E., S. M. Braaten, and B. E. Christensen. (2002) *J. Chromatogr. A*, **942**, 191.
[153] Fredheim, G. E., S. M. Braaten, and B. E. Christensen (2003). *J. Wood Chem. Technol.*, **23**, 197.
[154] Edelman, M. W., R. H. Tromp, and E. van der Linden. (2003) *Phys. Rev. E.*, **67**, 021404.
[155] Skendi, A., C. G. Biliaderis, A. Lazaridou, and M. S. Izydorczyk. (2003). *J. Cereal Sci.*, **38**, 15.
[156] Peng, Y. and L. Zhang. (2003) *J. Biochem. Biophys. Methods*, **56**, 243.

[157] Zhang, M., L. Zhang, P. C. K. Cheung, and J. Dong. (2003) *J. Biochem. Biophys. Methods*, **56**, 56.
[158] Žigon, M. and E. Ema Žagar. (2001) *Int. J. Polym. Anal. Charact.*, **6**, 521.
[159] Cathala, B., B. Saake, O. Faix, and B. Monties. (2003) *J. Chromatogr. A*, **1020**, 229.
[160] Tromp, R. H., E. ten Grotenhuis, and C. Olieman. (2002) *Food Hydrocoll.*, **16**, 235.
[161] Porsch, B., M. Andersson, B. Wittgren, and K.-G. Wahlund. (2002) *J. Chromatogr. A*, **946**, 69.
[162] Blagodatskikh, I. V., M. V. Sutkevich, N. L. Sitnikova, T. A. Pryakhina, O. E. Philippova, and A. R. Khokhlov, N. A. Churochkina. (2002) *J. Chromatogr. A*, **976**, 155.
[163] Kazmierski, M. and M. Corredig. (2003) *Food Hydrocoll.*, **17**, 685.
[164] Mleko, S., P. Janas, T. Wang, and J. A. Lucey. (2003) *Int. J. Dairy Technol.*, **56**, 157.
[165] Wang, T. and J. A. Lucey. (2003) *J. Dairy Sci.*, **86**, 3090.
[166] Ahrer, K., A. Buchacher, G. Iberer, D. Josic, and A. Jungbauer. (2003) *J. Chromatogr A*, **1009**, 89.
[167] Oliva, A., A. Santoveña, J. Fariña, and M. Llabrés. (2003) *J. Pharm. Biomed Anal.*, **33**, 145.
[168] Fowler, S., O. Byron, K. Jumel, D. Xing Zing, M. J. Corbel, and B. Bolgiano. (2003) *Vaccine*, **21**, 2678.
[169] Fraser, G. M., B. González-Pedrajo, J. R. H. Tame, and R. M. Macnab. (2003) *J. Bacteriology*, **185**, 5546.
[170] Hayashi, Y., H. Matsui, and T. Takagi. (1989) *Methods Enzymol.*, **172**, 514.
[171] Wen, J., T. Arakawa, and J. Philo. (1996) *Anal. Biochem.*, **240**, 155.
[172] Kendrick, B. S., B. A. Kerwin, B. S. Chang, and J. S. Philo. (2001) *Anal Biochem.*, **299**, 136.
[173] Yernool, D., O. Boudker, E. Folta-Stogniew, and E. Gouaux. (2003) *Biochem.*, **42**, 12981.
[174] Zhang, L., X. Li, Q. Zhou, X. Zhang, and R. Chen. (2002) *Polym. J.*, **34**, 443.
[175] van de Velde, F., H. S. Rellema, N. V. Grinberg, T. V. Burova, V. Y. Grinberg, and R. H. Tromp. (2002) *Biopolymers*, **65**, 299.
[176] Berggren, R., F. Berthold, E. Sjöholm, and M. Lindström. (2003) *J. Appl. Polym. Sci.*, **88**, 1170.
[177] Hokputsa, S., K. Jumel, C. Alexander, and S. E. Harding. (2003) *Eur. Biophys. J.*, **32**, 450.
[178] Mendichi, R., A. G. Schieroni, G. Cavallaro, M. Licciardi, and G. Giammona. (2003) *Polymer*, **44**, 4871.
[179] Lusignan, C. P., T. H. Mourey, J. C. Wilson, and R. H. Colby. (1995) *Phys. Rev. E.*, **52**, 6271.
[180] Lee, B. P., J. L. Dalsin, and P. B. Messersmith. (2002) *Biomacromolecules*, **3**, 1038.
[181] Matsumoto, A., S. Asai, S. Shimizu, and H. Aota. (2002) *Eur. Polym. J.*, **38**, 863.
[182] Meyer, A., N. Jones, Y. Lin, and D. Kranbuehl. (2003) *Macromolecules*, **35**, 2784.
[183] Xie, T., J. Penelle, and M. Verraver. (2002) *Polymer*, **43**, 3973.
[184] Podzimek, S. (2001) *Int. J. Polym. Anal. Charact.*, **6**, 533.
[185] Striegel, A. M. and D. B. Alward. (2002) *J. Liq. Chromatogr. Relat. Technol.*, **25**, 2003.
[186] Striegel, A. M. (2002) *Anal. Chem.*, **74**, 3013.
[187] Striegel, A. (2003) *Polym. Int.*, **52**, 1863.
[188] Girod, S., P. Baldet-Dupy, H. Maillols, and J.-M. Devoisselle. (2002) *J. Chromatogr. A*, **943**, 147.
[189] Wyatt, P. J. (2002) U.S. Patent 6,411,383 B1.
[190] Bloustine, J., V. Berejnov, and S. Fraden. (2003) *Biophys. J.*, **85**, 2619.